INCREMENTAL STRESS–STRAIN RELATIONSHIPS FOR REGULAR PACKINGS MADE OF MULTI-SIZED PARTICLES

CHING S. CHANG. ANIL MISRA and JIA H. XUE
Department of Civil Engineering. University of Massachusetts. Amherst. MA 01003. U.S.A.

Abstract—The mechanical behavior of a granular system is greatly influenced by its packing geometry. In this work, the concept of "Voronoi polyhedron" is utilized to characterize granular packings and it is shown that polyhedral tessellations can be used to represent packings of multi-sized particles. A stress–strain theory, based on micro-mechanical considerations, for small deformations of such packings is then described. The derived stress–strain relationship is compared with experimental results.

INTRODUCTION

Mechanical behavior of granular systems is of great importance in the areas of soil mechanics, powder mechanics, bulk solid mechanics and other related fields. The study of overall macroscopic behavior of granular systems in terms of continuum macroscopic field variables should be carried out with careful microscopic considerations. Earlier attempts at developing stress–strain relationships under small deformations were limited to simple regular packings of equal-sized spheres (Deresiewicz, 1958; Duffy and Mindlin, 1957; Makhlouf and Stewart, 1967), following the procedure outlined by Duffy and Mindlin (1957). This procedure considers a cubical representative cell and defines stress and strain for this cell in a conventional manner. However, for more complicated packing configurations which do not exhibit cubic symmetry the choice of cubic representative cell becomes difficult (Makhlouf and Stewart, 1967). For such packings the definition of stress and strain from conventional approach becomes cumbersome.

In this work, a method to the solution of stress–strain relations applicable to regular packings of equal-sized particles with frictional contacts (Chang, 1987) is extended to regular packings made of multi-sized particles. Polyhedral tessellations made of more than one "Voronoi cell" are used to represent such packings. The formulation of the stress–strain relationship is described and the results are compared with experimental data observed from tests performed on samples of cylindrical rods.

MICRO-STRUCTURAL CHARACTERIZATION

Granular systems consist of particles and associated voids arranged in space. To study the micro-geometrical structure of such systems, the concept of "Voronoi polyhedron" is used. The packing can be completely divided into polyhedral cells such that each of these cells contains one particle and its associated void space (Finney, 1970).

Packings of equal-sized particles

For a packing of equal spheres or discs, the "Voronoi cell" for a particle is defined as the smallest polyhedron constructed of a set of planes which are perpendicular bisectors of the vectors joining the center of the particle to the centers of its neighbors, such that no further plane cuts the polyhedron.

A regular packing of equal-sized particles can be represented by an unique "Voronoi cell", that is the packing can be constructed by repetitively stacking up this cell. Examples of "Voronoi cells" for some two-dimensional regular packings are shown in Fig. 1. The void ratio of this cell, the ratio of void volume to the solid volume in this cell, equals the void ratio of the packing. The coordination number (that is the number of contacts per
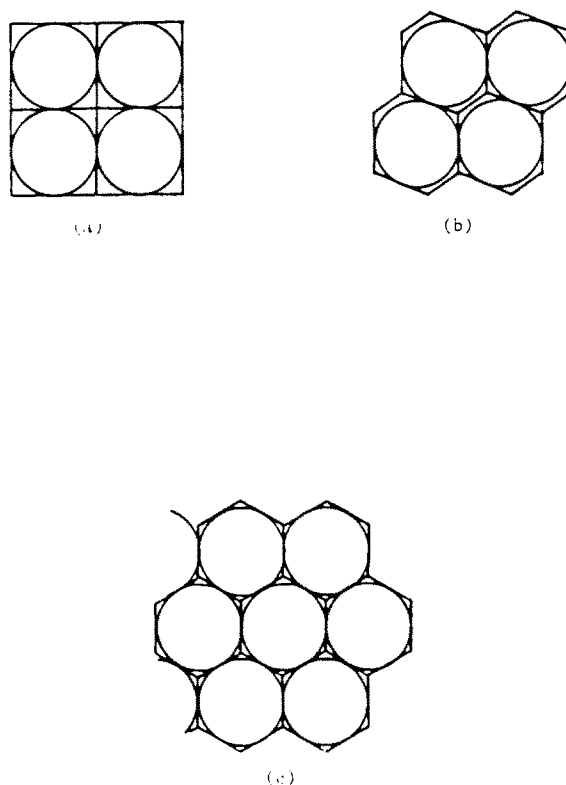
Fig. 1. Two-dimensional "Voronoi cells" for (a) square packing, (b) rhombic packing, and (c) hexagonal packing.

particle) of the cell equals the coordination number of the packing. Thus every polyhedron contains sufficient information to describe the void ratio and the coordination number of the packing and the neighborhood of the associated particle.

More complicated packing structures of equal-sized spheres cannot be represented by an unique "Voronoi cell". Such packings are termed "hypo-regular" packings in this work. These packings, in general, have multiple distinct "Voronoi cells" and the representative cell for such packings, therefore, has to be a polyhedron consisting of all these "Voronoi cells". This representative polyhedron of the packing is termed model tessellation of the packing in this work. The representative cell for a regular packing of equal particles is a particular case of model tessellation where the tessellation is made of only one "Voronoi cell".

Packings of multi-sized particles

For packings made of more than one size sphere or disc, the definition of "Voronoi cell" discussed in previous section is not appropriate, since it takes no regard of the particle size. For such packings, a generalization of the concept of "Voronoi polyhedron" called the radical plane polyhedron is used (Finney, 1983). The planes forming the radical plane polyhedron are such that they are perpendicular to the vector joining the centroids of the particle and its neighbor. However, unlike the case of equal-sized particles, these planes are not the bisector of the vector joining the centroids. The location of the plane can be determined as illustrated in Fig. 2 for the case of discs. The location of the plane is selected such that the plane passes through the point (O in Fig. 2) from which the tangent drawn to the particle and its neighbor are equal (that is OA = OB in Fig. 2). The "Voronoi cells" defined in this manner can be used to completely divide the packings of multi-sized particles.

From the above discussion it is clear that packings of multi-sized particles will have multiple distinct "Voronoi cells". Hence, the representative cell for such packings, as discussed in the previous section, will be a model tessellation.
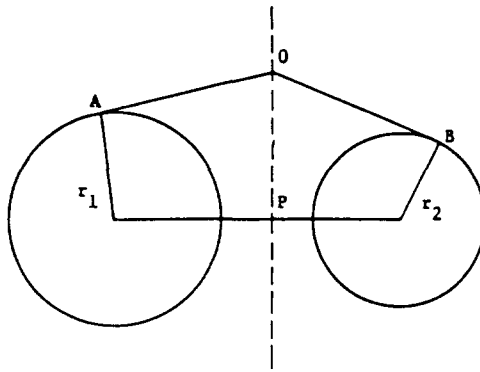
Fig. 2. Location of the plane forming the "Voronoi cell" for packings of multi-sized particles.

Tessellation

This section describes the structure of a model tessellation in more detail with the aid of some examples. Figure 3 shows examples of two hypo-regular packings and two packings of two-sized particles. The tessellations for these packings are shown by shaded areas in the figure. The model tessellation of a packing can be defined as the polyhedron consisting of all the possible shapes of "Voronoi cells" forming that packing. Such a tessellation will represent the packing, that is the packing can be constructed by repetitively stacking up this polyhedron. To keep the shape of the tessellation simple, the constituent "Voronoi cells" can be split. Thus, the choice of the tessellation to represent the packing can be made in several ways. For example, in Fig. 4(a) the "Voronoi cell" containing the small particle
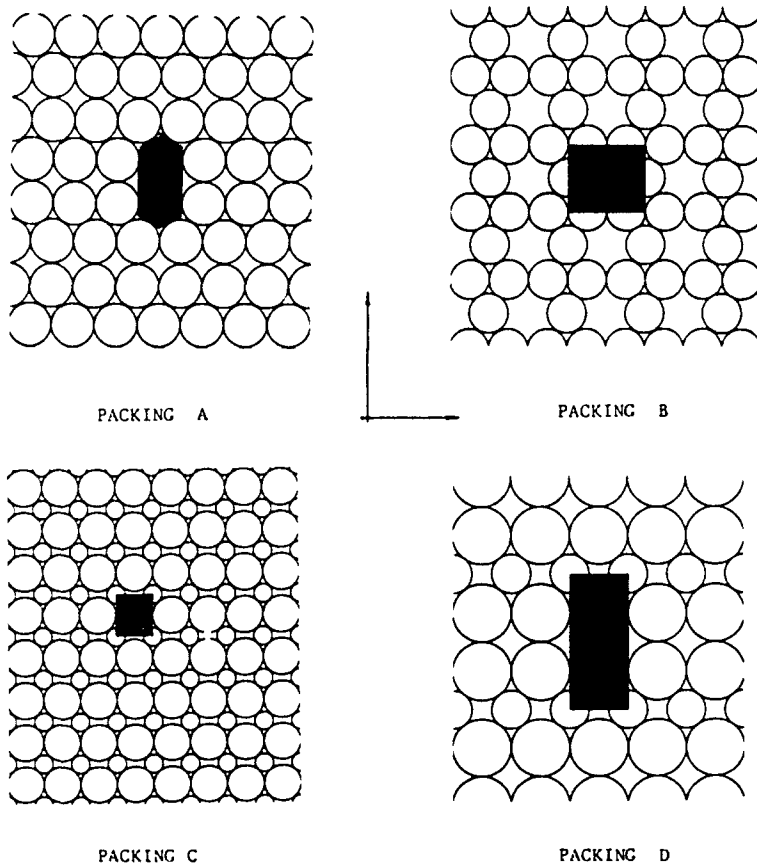

PACKING A

PACKING B

PACKING C

PACKING D

Fig. 3. Examples of "hypo-regular" packings (A and B) and packings of two-sized particles (C and D) in two dimensions.

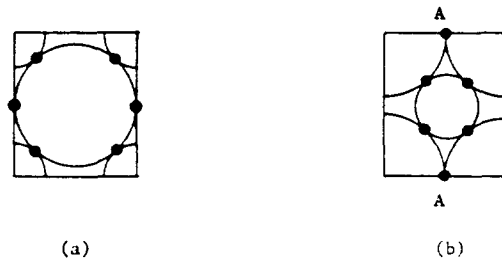(a)   (b)

Fig. 4. Two tessellations representing packing C of Fig. 3.

has been split into four and placed at diagonally opposite corners of the tessellation. This tessellation represents packing C in Fig. 3. Alternatively, the "Voronoi cell" containing the large particle can be split into four and placed at diagonally opposite corners of the tessellation as shown in Fig. 4(b). Note that the contact points lying on the boundary of the tessellation for a split particle (points A in Fig. 4(b)) are shared with the contiguous tessellation. For the packing C (see Fig. 3) the number of contacts for the large particle is 6 and the number of contacts for the small particle is 4, thus the average coordination number is 5. For the tessellation shown in Fig. 4(a), the number of contacts for the large particle is 6 and for the small particle is 4 (1 contact per quarter), thus the total number of contacts for the tessellation is 10 and the coordination number, as expected, is 5. For the tessellation shown in Fig. 4(b), the number of contacts for the large particle is 8 (2 contacts per quarter of large particle) and the number of contacts for the small particle is 4, thus the total number of contacts for the tessellation is 12. However, since the contacts A in Fig. 4(b) (two contact points at top A and two at bottom A) are shared, the average coordination number of the tessellation is 5 which is same as that of the packing. Furthermore, the void ratio (ratio of the area of voids to the area of solids) of the packing is same as the void ratio of its representative tessellations shown in Fig. 4(a) and (b).

STRESS STRAIN THEORY

In this section the theory developed for regular packings of equal-sized particles (Chang, 1987) is extended to packings of multi-sized particles and "hypo-regular" packings using model tessellation as the representative cell of the packing.

Stress tensor for the packing

According to the theorem of stress means (Truesdell and Toupin, 1960; Landau and Liphschitz, 1959), considering the static equilibrium and using the divergence theorem it can be shown that the stress tensor due to the boundary forces on the ath "Voronoi polyhedron" is given by

$$\sigma_{ij}^a = \frac{1}{V_a} \int_{V_a} \sigma_{ij} \, dV = \frac{1}{V_a} \int_{V_a} \sigma_{kj} r_{i,k} \, dV$$

$$= \frac{1}{V_a} \int_S \sigma_{kj} r_i n_k \, dS = \frac{1}{V_a} \int_S r_i t_j \, dS \tag{1}$$

or, for a discrete system,

$$\sigma_{ij}^a = \frac{1}{V_a} \sum_{m=1}^{N_a} r_i^{am} t_j^{am} \tag{2}$$

where V_a is the volume of the "Voronoi cell", N_a is the number of contacts in that "Voronoi cell", r_i^{am} is the vector joining the center of the ath particle to the mth contact, and t_j^{am} is the force at the mth contact of the ath particle. The tensor summation convention is assumed

for the subindices. Since a packing, in general, is made of multiple distinct "Voronoi cells", the stress field for the packing will generally be inhomogeneous. The average stress tensor for the packing is defined for the tessellation (representative cell) as a volume average quantity of stress, σ_{ij}^a, for the "Voronoi cells" comprising that tessellation. Thus

$$\hat{\sigma}_{ij} = \frac{1}{V} \sum_a \sigma_{ij}^a V_a \tag{3}$$

where $V = \sum_a V_a$ is the volume of the tessellation given by

$$V = V_s(1+e) \tag{4}$$

where V_s is the volume of the solid within the tessellation and e is the void ratio (ratio of the volume of voids to the volume of solids) of the tessellation. Introducing eqn (2) into eqn (3) it can be written that

$$\hat{\sigma}_{ij} = \frac{1}{V} \sum_a \sum_m r_i^{am} t_j^{am} \tag{5}$$

where the first summation is over all the Voronoi cells in the tessellation and the second over all the contacts in the ath Voronoi cell. Note that some of the contacts in the tessellation are shared with the neighboring tessellation (e.g. contact points A in Fig. 4(b)) and therefore the force at these contacts will also be shared. This should be appropriately accounted for the term t_j^{am} in eqn (5). Various forms of representations of stress tensor as a volume average of the contact forces have been suggested (Christoffersen et al., 1981; Kishino, 1978; Rothenburg and Selvadurai, 1981; Satake, 1978).

Since the size of the model tessellation is very small compared to the size of the packing, the stress tensor $\hat{\sigma}_{ij}$, introduced by the volume averaging process discussed above, can be considered to be same as Cauchy stress tensor of the continuum mechanics. Further, it can be shown that the average stress tensor $\hat{\sigma}_{ij}$ has all the properties of the Cauchy stress tensor (Rothenburg and Selvadurai, 1981). That is, the force f_i acting per unit area of a plane in the packing with a normal N is given by $f_i = \hat{\sigma}_{ij} N_j$ and that the stress tensor $\hat{\sigma}_{ij}$ satisfies the equation of static equilibrium. This definition of the stress tensor is used here to study the granular packing as a continuum media as it includes all the micro-geometrical characteristics of the packing.

Strain tensor for the packing

Similar to the stress tensor for the packing, in order to study the behavior of granular packing as a continuum media, there is a need to define a relationship between strain tensor and contact displacement. The particles in the assembly are considered to be rigid and conceptually connected with their contacting neighbors by deformable springs. It is assumed that the springs at the contacts are not destroyed during the deformation. The contact displacement refers to the deformation of the conceptual springs. From energy arguments, the work done described in terms of macro-variables, stress and strain, must equal the work done described in terms of micro-variables, force and displacement at the contacts. Equating the two works it gives

$$V\hat{\sigma}_{ij}d\bar{\varepsilon}_{ij} = \sum_a \sum_m t_j^{am} du_j^{am} ; \quad (i, j = x, y, z) \tag{6}$$

where $\hat{\sigma}_{ij}$ is the stress state of the tessellation, and $d\bar{\varepsilon}_{ij}$ is the corresponding incremental strain. t_j^{am} is the force acting on the point am (i.e. the mth contact of the ath particle), and du_j^{am} is the displacement of point am. Note that in the double summation in eqn (6) each contact is counted twice, once for each particle in contact. Thus the total deformation of the springs at contact m is $\mathbf{du} = \mathbf{du}^{am} + \mathbf{du}^{bm}$, where a and b are two particles in contact.

Substituting stress $\dot{\sigma}_{ij}$ in eqn (6) in terms of contact force r_i^{am} from eqn (5) and assuming that the work done at each contact described in terms of macro-variables is equal to that in terms of micro-variables, we obtain

$$r_i^{am} d\dot{\varepsilon}_{ij} = du_i^{am} \tag{7}$$

thus relating the strain tensor to the contact displacements. The underlying assumption here is that the strain field is homogeneous in the tessellation. Thus it is only applicable to the conditions where the strain is relatively uniform. Furthermore, the effects of large strains leading to the loss of contact are not considered in this analysis.

Local force–displacement relationship at a contact

For convenience, the displacement du_i^{am} in XYZ coordinate system can be transformed to du_j^{am} in the local coordinate system, *nst*, by a transformation tensor L_{ij}^m for the *m*th contact, thus

$$du_i^{am} = L_{ij}^{am} du_j^{am} \tag{8}$$

where the local coordinate system is constructed for each contact with three orthogonal unit vectors **n**, the unit vector normal to the contact point, **s**, and **t**. The vectors **s** and **t** are defined in Fig. 5 in the global XYZ coordinate system, where **s** is chosen to lie in the plane formed by **n** and Z. The angle β is measured on XY plane in a counter-clockwise direction from the positive X-axis and the angle α is measured from the positive Z-axis to the normal vector. Both α and β range from 0 to 180 degrees.

Similarly, the force vector r_i^{am} in the global coordinate system, XYZ, can be transformed to r_j^{am} in the local coordinate system. Thus eqn (5) becomes

$$\dot{\sigma}_{ij} = \frac{1}{V} \sum_a \sum_m r_i^{am} L_{ij}^{am} q_j^{am}. \tag{9}$$

The displacement du_j^{am} can be related to the incremental force dr_i^{am} at the *m*th contact by the following local constitutive law

$$dr_i^{am} = c_{ij}^{am} dw_j^{am} \tag{10}$$

where c_{ij}^{am} represents the stiffness constants for the springs connecting two particles in contact. For the contact of two non-conforming elastic bodies, c_{ij} are determined from contact theory as will be discussed later.
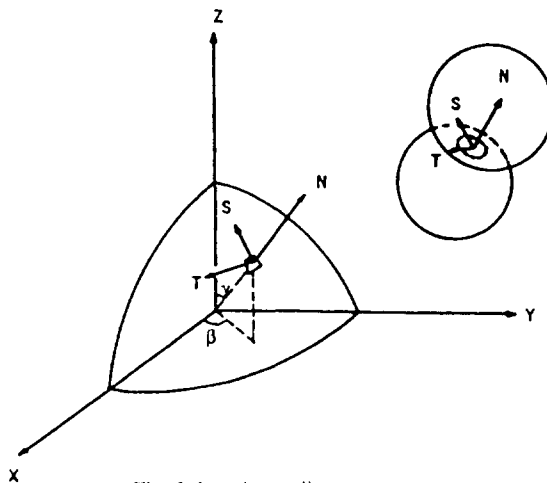

Fig. 5. Local coordinate system.

Constitutive equations of a packing

Introducing eqn (10) into eqn (8) and noting that $L_{il}L_{lj} = \delta_{ij}$ (Kronecker delta), it follows that

$$c_{IJ}^{am}L_{Jj}^{um}r_i^{um}d\bar{\varepsilon}_{ij} = dt_I^{um}. \tag{11}$$

Further, multiplying both sides by the transformation matrix L_{ql} and the position vector r_l, eqn (11) becomes

$$r_l^{am}L_{ql}^{um}c_{IJ}^{am}L_{Jj}^{um}r_i^{um}d\bar{\varepsilon}_{ij} = r_l^{am}dt_q^{um}. \tag{12}$$

Summing up on both sides, it can be written that

$$d\hat{\sigma}_{lq} = D_{lqij}\,d\hat{\varepsilon}_{ij} \tag{13}$$

where

$$D_{lqij} = \frac{1}{V}\sum_a \sum_m r_l^{um}L_{ql}^{um}c_{IJ}^{am}L_{Jj}^{um}r_i^{um} ; \quad \text{and}$$

$$d\hat{\sigma}_{lq} = \frac{1}{V}\sum_a \sum_m r_l^{um}dt_q^{um}. \tag{14}$$

Noting that the stress and the strain tensors are symmetric, the stiffness tensor must have the symmetries: $D_{lqij} = D_{qlij} = D_{lqji}$. Further, since the local stiffness tensor c_{IJ} is symmetric, the overall constitutive tensor satisfies the following: $D_{lqij} = D_{ijlq}$.

The incremental work done for the packing due to an increment of stress is the summation of the incremental work done at all contact points due to the consequent contact displacements. Thus the preservation of non-negativity of incremental energy for each contact point implies that the incremental energy for the packing is non-negative. In order to preserve a non-negative incremental energy for the packing, the contact force–displacement relationship should be adequately defined. In this study, the Mindlin contact theory is employed for the contact force–displacement relationship (Mindlin, 1949).

EXAMPLES

Based on the stress–strain developed in the preceding sections, the behavior of four packing configurations of cylinders (two-dimensional packings) is discussed in this section. Laboratory experimental tests were also performed on these packings. The experimental data obtained from these tests are compared with the theoretical predictions.

Packings

The packings chosen in this work are shown in Fig. 3. A and B are hypo-regular packings of equal diameter cylinders. C and D are packings made of two different-sized cylinders. The model tessellation (representative cell) of the packings is shown by the shaded portion of the packings. The void ratio e of the packings and the coordination number of the tessellation are also shown in Table 1. The ratio of the diameters of the two cylinders forming packing C is 2:1, and packing D is 2:1.5.

Table 1. Some geometrical properties of the four packings

Packing	Void ratio e	Coordination No.
A	0.1880	5.00
B	0.4702	4.00
C	0.1388	5.00
D	0.2154	4.67

Stress–strain matrix for the packings

For a two-dimensional case of packing of cylinders, the stress–strain relationship ((eqn (13)) derived in the preceding section can be written in Voigt's notation as

$$\begin{Bmatrix} \sigma_{xx} \\ \sigma_{yy} \\ \sigma_{xy} \end{Bmatrix} = \frac{1}{V} \begin{bmatrix} D_{11} & D_{12} & D_{13} \\ D_{21} & D_{22} & D_{23} \\ D_{31} & D_{32} & D_{33} \end{bmatrix} \begin{Bmatrix} \varepsilon_{xx} \\ \varepsilon_{yy} \\ 2\varepsilon_{xy} \end{Bmatrix}. \tag{15}$$

Two types of information are needed to evaluate D_{ij} in eqn (15), namely (1) packing geometry and (2) force–displacement relationship at the contact. The geometric properties for the packing, consisting of the volume of the tessellation and the coordinates of the contacts within a tessellation, have been discussed previously.

For a two-dimensional case of mating cylinders, the force–displacement relationship at a contact (eqn (10)) can be explicitly expressed as follows

$$\begin{Bmatrix} dt_n \\ dt_t \end{Bmatrix} = \begin{bmatrix} c_n & 0 \\ 0 & c_t \end{bmatrix} \begin{Bmatrix} du_n \\ du_t \end{Bmatrix} \tag{16}$$

where c_n and c_t are the contact normal and shear stiffnesses respectively. The normal stiffness c_n has been obtained by Hertz assuming that each cylinder is an elastic half space loaded by a parabolic pressure distribution. The Hertz theory was extended by Cattaneo (1938) and Mindlin (1949) to derive the relationship for tangential stiffness c_t (Johnson, 1985). Based on empirical data, modifications of these relationships have been suggested under conditions of local yielding at the contact (Misra, 1987). The modified relationships are given by

$$1/c_n = \frac{1-v}{2\pi \tilde{G}} [2 \ln (2r/\tilde{a}) - 1] \tag{17}$$

$$1/c_t = 1/c_n \Psi [1 - t_t/(\tan \phi_\mu t_n)]^{-1/2} \tag{18}$$

where $\tilde{a} = (2(1-v)t_n r/\pi \tilde{G})^{1/2}$, $\tilde{G}$ is an equivalent shear modulus which is less than the elastic shear modulus when local yielding occurs, v is the Poisson's ratio, r is the equivalent radius of the particles given by

$$\frac{1}{r} = \frac{1}{2}\left[\frac{1}{r_1} + \frac{1}{r_2}\right], \tag{19}$$

ϕ_μ is the friction angle between the two particles, t_n and t_t are the normal and shear force at the contact respectively, Ψ is a constant, r_1 and r_2 are the radius of the two mating cylinders. It is noted that for Ψ equal to 1 the above equation reduces to that suggested by Mindlin.

Comparison with experimental results

The experimental setup consists of a loading frame so designed as to be able to apply both normal and shear loading on a sample of cylindrical rods placed inside it. The rod assembly is placed on a glass table top such that the cylinders stand vertically on the table. The sample consists of an assembly of approximately 300 aluminum cylinders, of 2 in. (5.08 cm) height, placed in accordance with a given packing arrangement. For equal-sized packings, packings A and B, the diameter of the cylinders used was 0.5 in. (1.25 cm). For packings C, the diameter of the cylinders used were 0.5 in. (1.25 cm) and 0.25 in. (0.625 cm) and for packing D, 0.75 in. (1.875 cm) and 0.5 in. (1.25 cm). Two factors may influence the measured data, namely the flexibility of the loading frame and the friction at the bottom
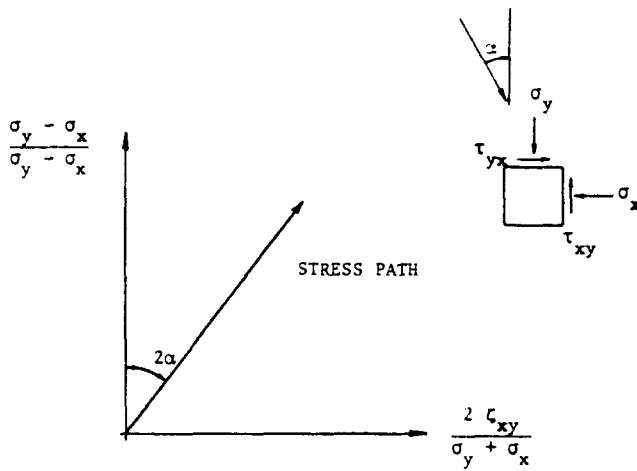
Fig. 6. Loading path followed for the experimental tests plotted on a normalized stress plane.

of rod assembly. Since the loading frame used is relatively rigid with respect to the rod assembly and since for all the tests the stress magnitude is much larger than the friction at the bottom, the effect of these factors is expected to be insignificant. However, calibration was carried out to account for these in the test results (Xue, 1988). The loading conditions followed for the tests are illustrated in Fig. 6 on a normalized deviatoric stress vs shear stress plot. All the tests have an isotropic initial stress state, represented by the point of origin in Fig. 6. An initial isotropic stress at 2.5 psi (17.24 kN/m²) is used for all the tests. Tests were performed for various values of angle α, which is the inclination of the principal stress axis to the chosen material axis (Y-axis in Fig. 3). All the tests were performed several times and fairly repeatable test results were obtained.

To compare with the experimental results, the response of the four packings under the loading conditions discussed above were computed using the theory. The values of the constants used for theoretical computations in this work are: $\tilde{G} = 15000$ psi (105000 kN/m²), $\Psi = 2.5$, $v = 0.1$, and $\phi_\mu = 15°$. The measured results are plotted along with the predicted theoretical results as shown in Fig. 7(a–d) for the four packings, respectively. The observed scatter in the measured results is consistent with the repeatability of the tests.

Figure 8(a–d) shows the effect of rotation of the principal stress axis on the stress–strain response of the four packings, respectively. The measured results are plotted along with the predicted theoretical results for the various values of α on a normalized strain axis. With increase in α, the ratios $\gamma_{xy}/\varepsilon_v$ and $\varepsilon_x/\varepsilon_y$, as expected, increase for all the packings. A fairly good agreement is obtained between the measured and the predicted results.

Investigation of the strain increment direction shows that the four packings exhibit different behavior of non-coaxiality between stress and strain increment directions. Figure 9(a–d) shows the angle of non-coaxiality plotted against the stress direction α for the two packings. The measured values are plotted along with the theoretical results. It is noted that small variation in the measured values of strains can cause large differences in the non-coaxiality angle. Thus, considering the scatter in the measured data, the agreement obtained between the theoretical and the experimental values of the non-coaxiality angles is reasonably good.

In addition to the deformation response of the packings the contact forces within the tessellation are also computed. As an example, the contact forces within the tessellation (see Fig. 4(b)) for packing C are shown. Figure 10(a) shows the contact forces for the initial isotropic stress state. It can be seen that for an overall isotropic stress state there are shear forces on the contacts. Figure 10(b) shows the contact forces for the same tessellation after a load increment in the direction of $\alpha = 45°$. It can be observed that for this packing all the particles in the tessellation are in equilibrium. However, because of the volume averaging process in the formulation, the force and moment equilibrium for individual particles are not guaranteed.
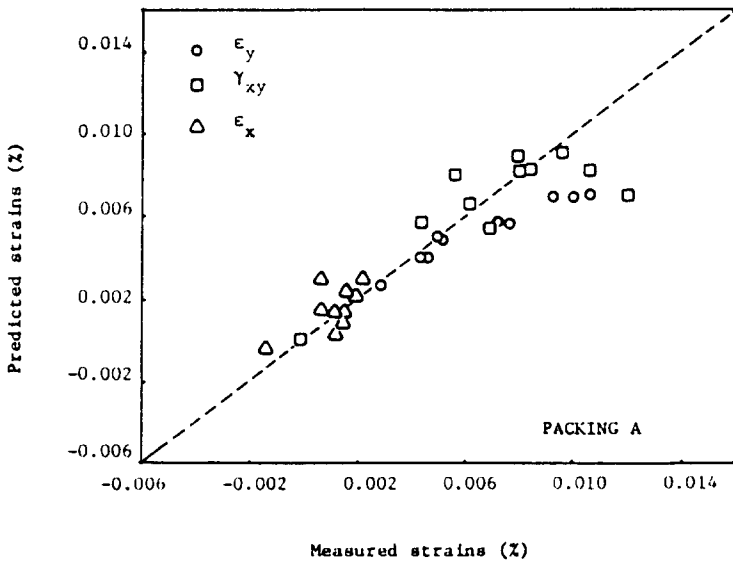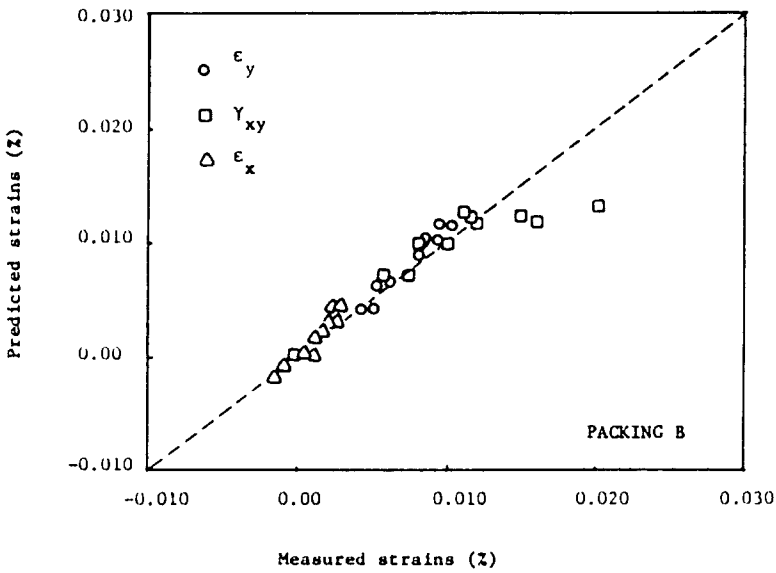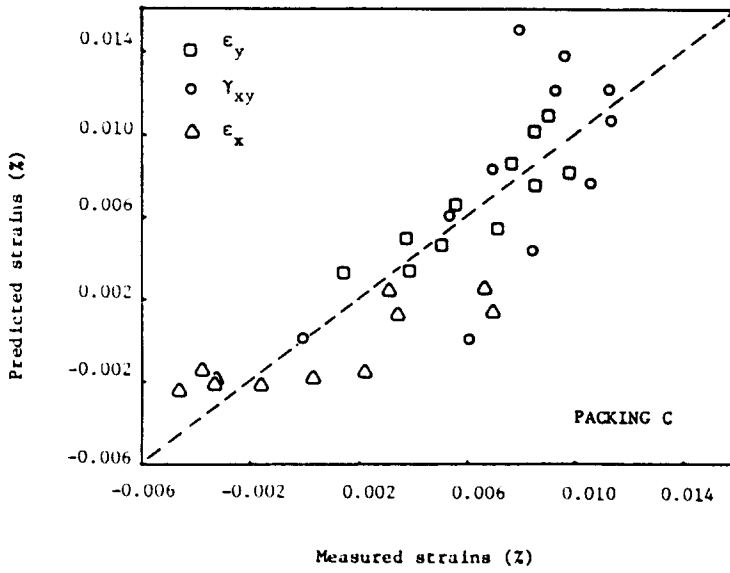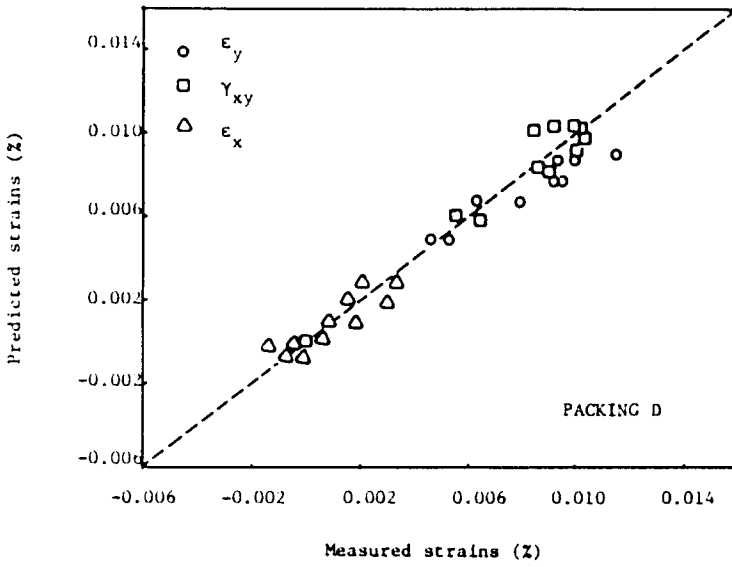
Fig. 7(a).

Fig. 7(b).

Fig. 7(c).

Fig. 7(d).

Fig. 7. Comparison of measured and predicted strains for (a) packing A ; (b) packing B ; (c) packing C ; (d) packing D.
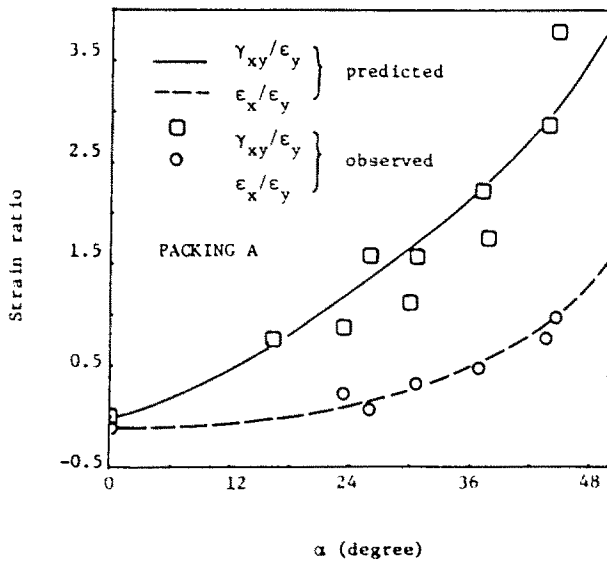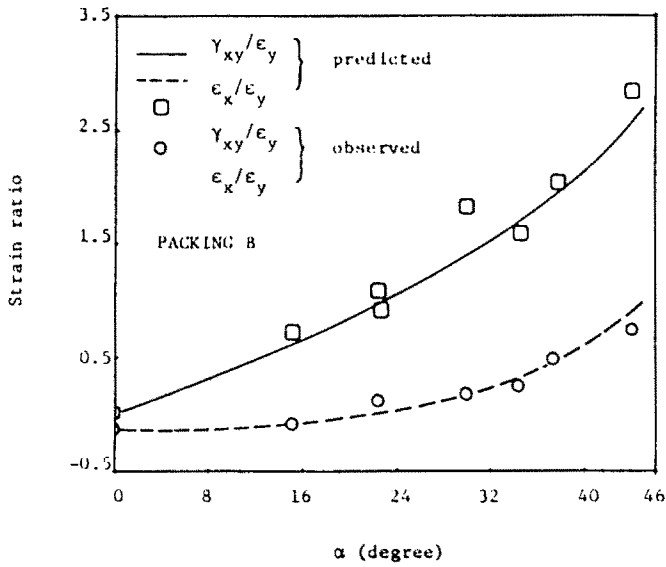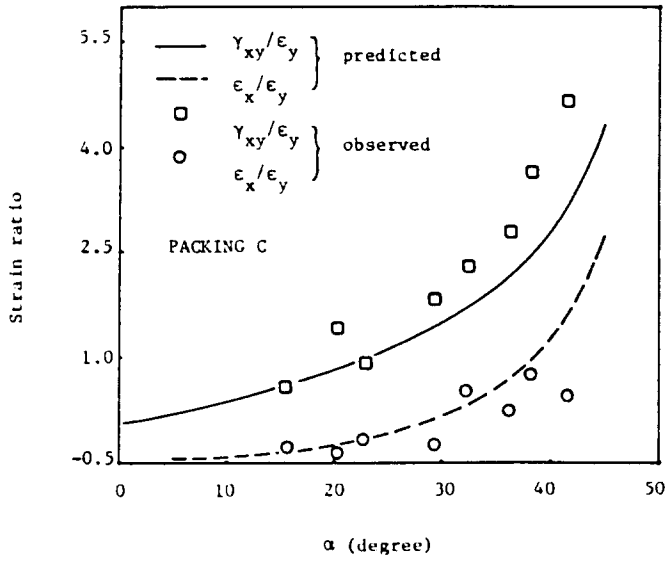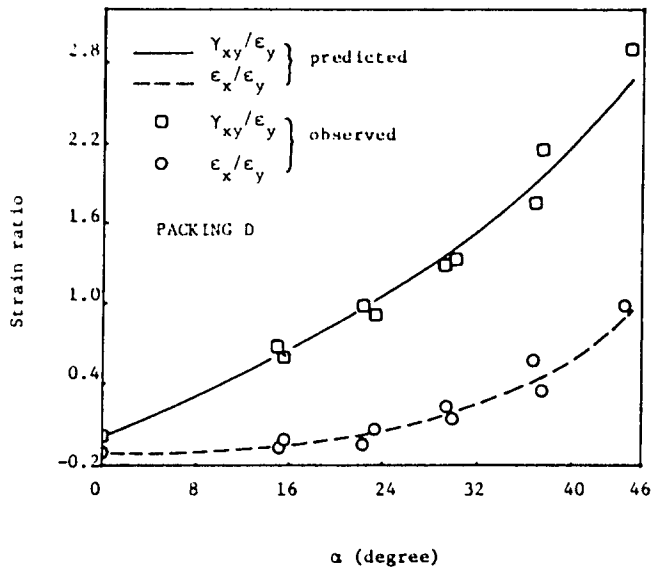
Fig. 8(a).

Fig. 8(b).

Fig. 8(c).

Fig. 8(d).

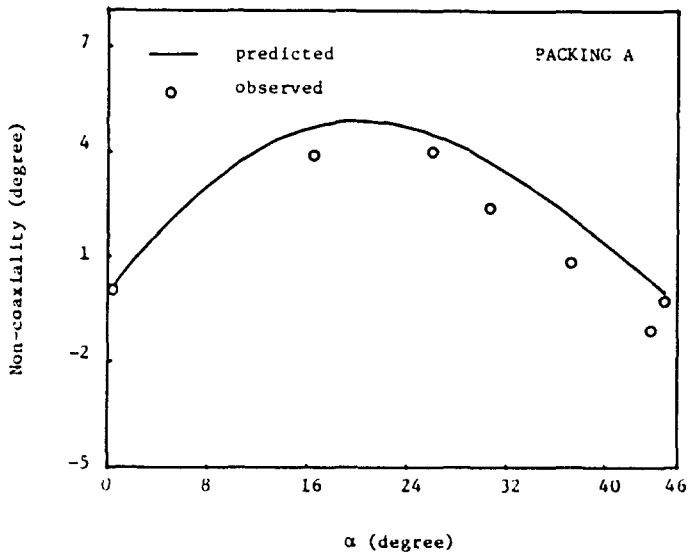Fig. 8. Measured and predicted strain ratios plotted against loading direction α for (a) packing A; (b) packing B; (c) packing C; (d) packing D.
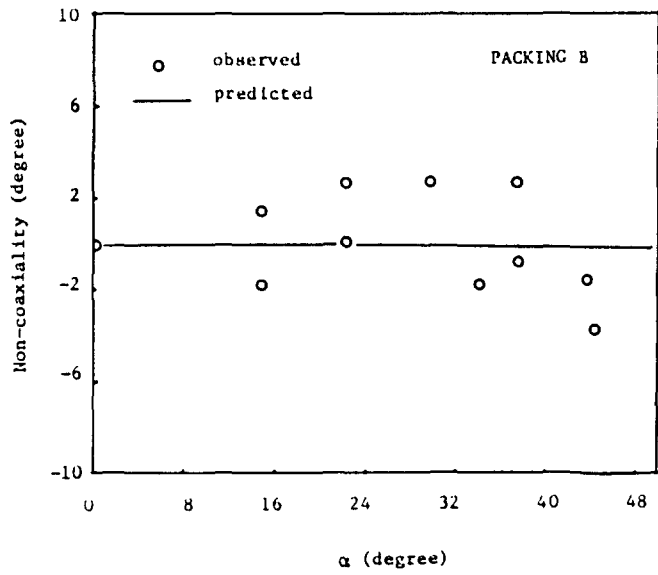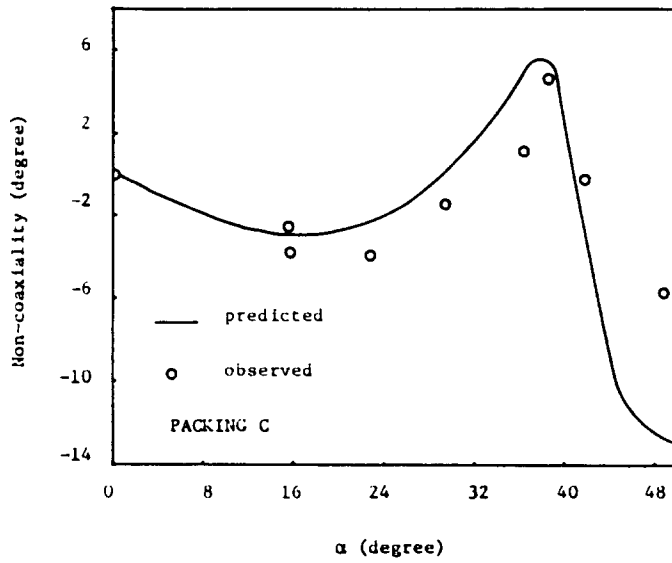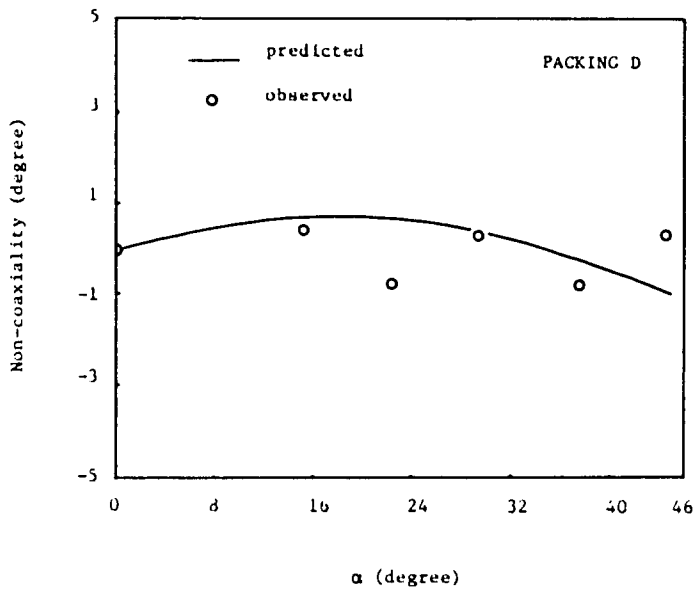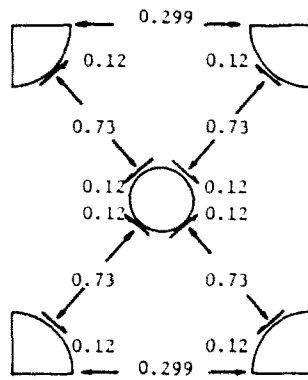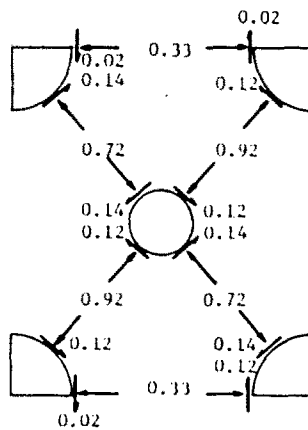
Fig. 9(a).

Fig. 9(b).

Fig. 9(c).

Fig. 9(d).

Fig. 9. Measured and predicted non-coaxiality angle plotted against loading direction α for (a) packing A; (b) packing B; (c) packing C; (d) packing D.

(a)

(b)

Fig. 10. Contact forces within the tessellation for packing C.

CONCLUDING REMARKS

From the experimental results and the theoretical predictions it is apparent that packing arrangement has great influence on the stress–strain behavior of the granular systems. The comparison of the results shows that the developed theory can properly account for the effect of packing arrangement on the deformation response.

REFERENCES

Cattaneo, C. (1938). Sul contatto di due corpi elasti. *Academia dei Lincei, Rendiconti*, Ser. 6, 27, 342–348, 434 436, 474–478.

Chang, C. S. (1987). Micromechanical modelling of constitutive relations for granular material. *Proc. US–Japan Seminar on Micromechanics of Granular Materials* (Edited by J. T. Jenkins and M. Satake), pp. 271–278. Elsevier, Amsterdam.

Christoffersen, J., Mehrabadi, M. M. and Nemat-Nasser, S. (1981). A micromechanical description of granular material behavior. *J. Appl. Mech.* 48, 339–344.

Deresiewicz, H. (1958). Stress–strain relations for a simple model of a granular medium. *J. Appl. Mech.* 25, 402–406.

Duffy, J. and Mindlin, R. D. (1957). Stress–strain relations and vibrations of granular media. *J. Appl. Mech.* 24, 585–593.

Finney, J. L. (1970). Random packings and structure of simple liquids. I. The geometry of random close packing. *Proc. R. Soc.* A, 319, 479–493.

Finney, J. L. (1983). Structure and properties of granular materials: guidelines for modelling studies of liquids

and amorphous solids. In *Advances in the Mechanics and the Flow of Granular Materials* (Edited by M. Shahinpoor). Ch. II, pp. 19–37. Gulf Publishing, Houston, TX.

Johnson, K. L. (1985). *Contact Mechanics*. Cambridge University Press, London.

Kishino, Y. (1978). Statistical consideration on deformation characteristics of granular materials. In *Proc. US–Japan Seminar on Continuum Mechanical and Statistical Approaches in the Mechanics of Granular Materials* (Edited by S. C. Cowin and M. Satake), pp. 114–122.

Landau, L. D. and Liphschitz, E. M. (1959). *Theory of Elasticity*. Pergamon Press, London.

Makhlouf, H. and Stewart, J. J. (1967). Elastic constants of cubical-tetrahedral and tetragonal sphenoidal arrays of uniform spheres. In *Proc. International Symposium of Wave Propagation and Dynamic Properties of Earth Materials*, Albuquerque, NM, pp. 825–837.

Mindlin, R. D. (1949). Compliance of elastic bodies in contact. *J. Appl. Mech.* 16, 259–268.

Misra, A. (1987). Stress–strain relationships for simple models of sands. Report No. OUR-87-02/UMASS, submitted to University of Massachusetts in partial fulfillment of the requirements of the degree of Master of Science.

Rothenburg, L. and Selvadurai, A. P. S. (1981). Micromechanical definition of the Cauchy stress tensor for particulate media. In *Mechanics of Structured Media* (Edited by A. P. S. Selvadurai), pp. 469–486. Elsevier.

Satake, M. (1978). Constitution of mechanics of granular materials through the graph theory. *Proc. US–Japan Seminar on Continuum Mechanical and Statistical Approaches in the Mechanics of Granular Materials* (Edited by S. C. Cowin and M. Satake), pp. 47–62.

Truesdell, C. and Toupin, R. A. (1960). The classical field theories. In *Handbuch der Physik* (Edited by S. Flugge), Vol. III 1. Springer, Berlin.

Xue, J. H. (1988). Experimental studies on mechanical behavior of idealized granular media. Report No. OUR-88-01 UMASS, submitted to University of Massachusetts in partial fulfillment of the requirements of the degree of Master of Science.